

# Hierarchical Recursive Precision for Accelerating Symmetric Linear Solves on MXUs

Vicki Carrica<sup>1</sup>, Rabab Alomairy<sup>1</sup>, Evelyne Ringoot<sup>1</sup>, and Alan Edelman<sup>1</sup>

CS and AI Laboratories, Massachusetts Institute of Technology, Cambridge, MA,  
USA

{vickicar,rabab53,eringoot,edelman}@mit.edu

**Abstract.** Symmetric positive-definite system solvers based on Cholesky factorization are fundamental to many scientific applications, such as climate modeling. We present a portable, nested recursive mixed-precision solver designed for Matrix Processing Units (MXUs), including NVIDIA Tensor Cores (H200) and AMD Matrix Cores (MI300X), that assigns low-precision FP16 arithmetic to large off-diagonal blocks, while preserving high precision on diagonal blocks to ensure numerical stability. The solver is implemented in Julia, providing a high-level, hardware-agnostic interface. We demonstrate a speedup of  $5.32\times$  versus double precision cuSOLVER, with  $100\times$  better accuracy than pure half precision on H200, providing higher accuracy than low-precision at higher speed than high-precision. Comparable results are observed on MI300X, demonstrating broad applicability across GPUs.

**Keywords:** Cholesky decomposition · mixed precision · recursive algorithms · GPU acceleration · symmetric positive definite matrices · triangular solve (TRSM) · symmetric rank-k update (SYRK) · tensor cores · matrix processing units (MXUs) · Julia language · quantization.

## 1 Introduction

Symmetric linear systems are a critical performance bottleneck in large simulations, for example, computational fluid dynamics [33, 36], climate modeling [2], and Gaussian process regression [25]. Direct solution methods of such symmetric linear systems involve calculating their Cholesky decomposition, which relies on triangular solve (TRSM) and symmetric rank-k update (SYRK). These systems have traditionally been solved in uniform high precision, limiting their ability to exploit novel AI accelerators, with lower-precision Matrix Processing Units (MXUs), such as NVIDIA Tensor Cores and AMD Matrix Cores [16]. Deploying these capabilities in high-precision scientific computing requires a mixed-precision approach where high accuracy and improved speed are combined.

Our solution for mixed-precision builds upon the well-known *recursive subdivision strategy* [8, 13, 22], which enhances data locality and parallelism in Cholesky factorization. While prior recursive formulations typically apply only to the diagonal POTRF operation—leaving off-diagonal updates (TRSM and

SYRK) in standard blocked form—we extend this into a fully *nested recursive formulation*. In our approach, the decomposition tree recursively subdivides not only POTRF but also TRSM and SYRK, resulting in a structure that breaks the matrix at each level into two recursive POTRFs, one TRSM, and one SYRK, further increasing the granularity of GEMM operations [17]. We integrate this in a *tree-structured mixed-precision hierarchy* that assigns low precision (FP16) to large off-diagonal blocks and progressively higher precision (FP32 or FP64) to recursively refined diagonal regions. This contrasts with most prior mixed-precision approaches, which either focus on iterative refinement [19,29] or apply uniform low precision to predefined matrix partitions [31,38]. To mitigate FP16’s limited dynamic range, we apply lightweight *per-block quantization and dequantization*, preserving numerical stability with minimal overhead. We focus in this work on diagonally dominant problems, for which this is a reasonable strategy. For non-diagonally dominant problems, other mixed-precision strategies need to be considered. The solver is implemented as a layered mixed-precision scheme in Julia.

The main contribution of this work is the integration of a tree-based mixed-precision scheme into a multi-stage recursive subdivision strategy in a unified portable data structure, demonstrating significant speedups of mixed-precision approaches over high-precision vendor libraries on a single GPU, while maintaining higher accuracy than low precision. On NVIDIA H200 GPUs, our solver achieves a  $5.32\times$  speedup over FP64 cuSOLVER, and a  $5.07\times$  speedup against cuSOLVER FP32, with  $100\times$  better accuracy than pure FP16 and 88% of Pure FP16’s peak throughput. Similar trends are observed on AMD MI300X, showcasing the cross-platform scalability and practicality of our approach.

## 2 Background

### 2.1 Recursive Decomposition

Recursive formulations have long been studied as a strategy to improve data locality and expose parallelism in dense linear algebra. Dense linear algebra algorithms such as the Cholesky decomposition are often bounded by communication cost, rather than arithmetic cost, motivating the development of communication-avoiding Cholesky implementations [11]. Early efforts in dense matrix settings—such as [8,22]—proposed recursive blocked factorizations, and recursive formulations for hierarchical low-rank solvers [21,27], where recursion is limited to the diagonal factorization, with off-diagonal updates computed via standard blocked methods following LAPACK-style parallelism [9]. Other frameworks, such as libflame [37], also developed hierarchical approaches for dense linear algebra. More recently, optimizing task granularity in hybrid CPU-GPU environments has been done through recursive task graphs [23,24,34]. Recursive TRSM has been explored more in the GPU setting. Charara et al. [20] introduced a recursive triangular solver designed to exploit data locality and task decomposition on GPU architectures. In the context of high-level portable programming, Carrica et al. [17] implemented a recursive GPU TRSM in Julia, demonstrating

its benefits on tensor-core hardware. To the best of our knowledge, our work is the first to propose and evaluate a *recursive GPU-based SYRK* extending across all three phases —POTRF, TRSM, and SYRK—, along with a mixed-precision variant that strategically exploits low-precision GEMM acceleration.

## 2.2 Mixed-Precision Linear Algebra

Mixed-precision techniques have gained significant attention as a means to accelerate numerical algorithms while reducing energy consumption. Higham et al. [29], along with others [4, 10, 14, 18, 19, 28] studied mixed-precision iterative refinement for dense and sparse systems. More recently, task-based and batched GPU solvers have explored integrating low-precision arithmetic at the kernel level [3, 6, 31, 38], often relying on uniform block-level precision assignment. Other approaches apply precision dynamically based on sub-matrix norms [15] or use non-uniform thresholds for block low-rank LU factorization [7]. Our work extends these ideas by introducing a *tree-structured precision hierarchy*, assigning FP16 to large off-diagonal blocks and higher precision (FP32 or FP64) to recursively refined diagonal regions. This enables controlled use of MXU-accelerated low-precision GEMM operations without compromising stability. Our approach also integrates lightweight per-block quantization and dequantization [30], ensuring robustness when operating near FP16’s dynamic range limits, which will be described in Section 3.3. To our knowledge, this is the first work to unify recursive decomposition and layered mixed-precision execution in a single portable solver framework, targeting both NVIDIA and AMD matrix engines.

## 2.3 Julia Language abstractions

The implementation of a recursive mixed-precision Cholesky solver is facilitated by the Julia programming language [12]. Julia’s multiple dispatch and type inference with compile-time specialization permits writing single hardware-agnostic calls to specialized core operations—POTRF, TRSM, SYRK, and GEMM—which the compiler then resolves and optimizes automatically based on data type (e.g., FP16, FP32, FP64), enabling a unified mixed-precision recursive solver framework, combining portability and high performance [5, 26, 35]. In previous work, a full-cycle low-level implementation of TRSM and TRMM, directly compiled to GPU machine language, was demonstrated to provide performance on par with vendor-optimized functions [17]. In the current work, we focus on the recursive implementation of Cholesky, and lean on low-level vendor library implementation of POTRF, TRSM, SYRK, and GEMM through multiple dispatch for the base cases. This algorithm could in the future be a critical building block towards the performant low-level hardware-agnostic implementation of Cholesky decomposition for small and large data sizes for all GPU hardware.

### 3 Methods

#### 3.1 Nested Recursive Algorithm Design

We implement a nested recursive Cholesky algorithm that decomposes symmetric positive-definite (SPD) matrices by hierarchically breaking down all three core computational phases: POTRF (Cholesky factorization), TRSM (triangular solve), and SYRK (symmetric rank- $k$  update). By replacing standard TRSM and SYRK updates with their recursive counterparts, we expose more parallelism and achieve deeper task granularity. This structure increases arithmetic intensity and enables greater utilization of BLAS-3 routines, particularly GEMM, which are highly optimized on modern GPU architectures with MXUs.

For TRSM, this form of recursion was first introduced for GPUs in [20], and its portable Julia implementation was recently explored in [17].

---

**Algorithm 1** Tree-POTRF $_L(A, b)$ : Nested-recursive Cholesky (lower)

---

**Require:**  $A \in \mathbb{R}^{n \times n}$  SPD; leaf size  $b$

```

1: if  $n \leq b$  then
2:    $A \leftarrow \text{POTRF}_L(A)$ 
3:   return
4: end if
5: Choose  $n_1$  (e.g.  $n_1 = \lfloor n/2 \rfloor$ );  $n_2 = n - n_1$ 
6: Partition  $A = \begin{bmatrix} A_{11} & 0 \\ A_{21} & A_{22} \end{bmatrix}$ 
7: TREE-POTRF $_L(A_{11}, b)$   $\triangleright A_{11} \leftarrow L_{11}L_{11}^\top$ 
8: TREE-TRSM $_{R,L,T}(A_{21}, L_{11}, b)$   $\triangleright A_{21} \leftarrow A_{21}L_{11}^{-\top}$ 
9: TREE-SYRK $_L(A_{22}, A_{21}, \alpha = -1, \beta = 1, b)$   $\triangleright A_{22} \leftarrow A_{22} - A_{21}A_{21}^\top$ 
10: TREE-POTRF $_L(A_{22}, b)$ 

```

---

Algorithm 1 outlines the recursive Cholesky factorization for an SPD matrix  $A$  (see Figure 1). At each level, the matrix is split into a diagonal block  $A_{11}$  and a trailing submatrix  $A_{22}$ . The decomposition proceeds through four recursive stages: (1) diagonal POTRF on  $A_{11}$  (line 7), (2) triangular solve (TRSM) on the off-diagonal block (line 8), (3) symmetric rank- $k$  update (SYRK) on the trailing submatrix  $A_{22}$  (line 9), and (4) recursive POTRF on the updated  $A_{22}$  (line 10). Algorithm 2 applies TRSM recursively to solve  $B \leftarrow BL^{-T}$  for a lower-triangular matrix  $L$ . If the matrix size falls below the threshold  $b$ , a standard TRSM kernel is used (line 2). Otherwise,  $L$  and  $B$  are split, and the update  $B_2 \leftarrow B_2 - B_1L_{21}^\top$  is computed using GEMM (line 7). Similarly, Algorithm 3 performs the SYRK update  $C \leftarrow \beta C + \alpha AA^\top$  recursively. The off-diagonal contribution  $C_{21} \leftarrow \beta C_{21} + \alpha A_2A_1^\top$  is explicitly computed via GEMM (line 7), while the diagonal blocks are handled recursively.

#### 3.2 Hierarchical Mixed Precision on the recursion structure

This hierarchical recursion naturally supports our *layered mixed-precision scheme* integrated into our recursive Cholesky algorithm.

<p><b>Algorithm 2</b> Tree-TRSM<sub>R,L,T</sub>(<math>B, L, b</math>)</p> <p><b>Require:</b> <math>B \in \mathbb{R}^{m \times n}</math>, <math>L \in \mathbb{R}^{n \times n}</math> lower-tri; leaf <math>b</math></p> <ol style="list-style-type: none"> <li>1: <b>if</b> <math>\min(m, n) \leq b</math> <b>then</b></li> <li>2:     <math>B \leftarrow \text{TRSM}(\dots; L, B)</math></li> <li>3:     <b>return</b></li> <li>4: <b>end if</b></li> <li>5: <math>n_1 = \lfloor n/2 \rfloor</math>, Split <math>L = \begin{bmatrix} L_{11} &amp; 0 \\ L_{21} &amp; L_{22} \end{bmatrix}</math>, <math>B = \begin{bmatrix} B_1 &amp; B_2 \end{bmatrix}</math></li> <li>6: TREE-TRSM(<math>B_1, L_{11}, b</math>)</li> <li>7: <math>B_2 \leftarrow B_2 - B_1 L_{21}^\top</math></li> <li>8: TREE-TRSM(<math>B_2, L_{22}, b</math>)</li> </ol>	<p><b>Algorithm 3</b> Tree-SYRK<sub>L</sub>(<math>C, A, \alpha, \beta, b</math>)</p> <p><b>Require:</b> <math>C \in \mathbb{R}^{n \times n}</math> sym.; <math>A \in \mathbb{R}^{n \times k}</math>; leaf <math>b</math></p> <ol style="list-style-type: none"> <li>1: <b>if</b> <math>n \leq b</math> <b>then</b></li> <li>2:     <math>C \leftarrow \text{SYRK}(\dots; \alpha, A, \beta, C)</math></li> <li>3:     <b>return</b></li> <li>4: <b>end if</b></li> <li>5: <math>n_1 = \lfloor n/2 \rfloor</math>, Split <math>A = \begin{bmatrix} A_1 \\ A_2 \end{bmatrix}</math>, <math>C = \begin{bmatrix} C_{11} &amp; 0 \\ C_{21} &amp; C_{22} \end{bmatrix}</math></li> <li>6: TREE-SYRK(<math>C_{11}, A_1, \alpha, \beta, b</math>)</li> <li>7: <math>C_{21} \leftarrow \beta C_{21} + \alpha A_2 A_1^\top</math></li> <li>8: TREE-SYRK(<math>C_{22}, A_2, \alpha, \beta, b</math>)</li> </ol>
--	---

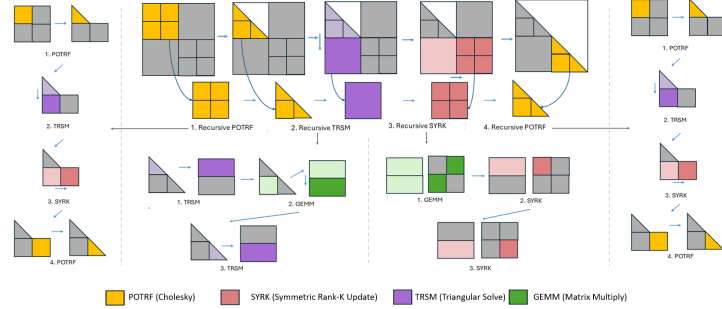
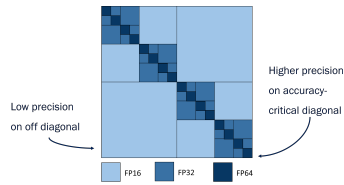


Fig. 1. Nested Recursive Cholesky Decomposition Tree

Specifically, we assign: (i) **Low precision (e.g., FP16)** to large, off-diagonal blocks that dominate the computation but are less sensitive to numerical error. These are typically updated using GEMM during TRSM and SYRK phases. (ii) **Higher precision (e.g., FP32 or FP64)** to diagonal blocks, which undergo POTRF and are more susceptible to round-off errors. These blocks contribute directly to the factorization’s stability and accuracy.

This layered precision design (Figure 2) maximizes performance while preserving overall stability. In the context of Cholesky, this assignment is particularly effective because the diagonally dominant matrices we target have the most numerically sensitive operations near the diagonal.

Our method is based on a custom recursive data structure implemented in Julia, which represents a symmetric matrix  $A$  as a tree of submatrices. In terms of memory usage, this algorithm requires no additional memory during computation. The hierarchical data structure relies entirely on matrix views to partition the data, and the recursive solver updates these blocks strictly in-place.



**Fig. 2.** Recursive data structure enabling layered mixed precision.

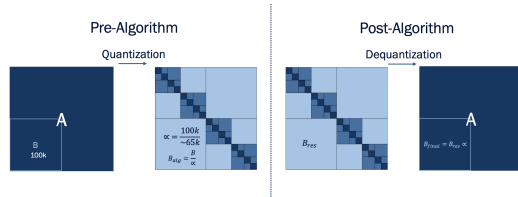


**Fig. 3.** Blockwise quantization and dequantization workflow.

### 3.3 Layered Quantization and Dequantization Strategy

To mitigate FP16’s limited dynamic range and avoid numerical overflow, we introduce a lightweight, per-block quantization and dequantization step at each level of the recursive tree. Prior to each low-precision GEMM operation, matrix blocks are rescaled into a dynamic range appropriate for FP16 execution, and then scaled back after the operation completes. Figure 3 illustrates this process.

Let  $A$  be the symmetric positive definite matrix to factorize, and  $B$  an associated data block (e.g., right-hand side or update block) with large dynamic range. To prevent overflow when operating in low precision, we explicitly manage the dynamic range relative to  $R_{\max}$ , the maximum representable finite value of the target format. We compute a scaling factor  $\alpha$  as  $\alpha = \max\left(1, \frac{\|B\|_{\infty}}{R_{\max}}\right)$ .

Prior to the algorithm, if the values in  $B$  exceed the range (i.e.,  $\frac{\|B\|_{\infty}}{R_{\max}} > 1$ ), this scaling compresses  $B_{\text{alg}}$  into the safe range  $[-R_{\max}, R_{\max}]$ . If the values are already within range,  $\alpha$  remains 1, and  $B_{\text{alg}}$  preserves the original scale. Upon algorithm completion on  $B_{\text{alg}}$ , we obtain an intermediate result  $B_{\text{res}}$ , which is dequantized:  $B_{\text{final}} = B_{\text{res}} \cdot \alpha$ . This quantization–dequantization process is embedded at each level of the recursive solver and is applied only to off-diagonal blocks. Combined with our tree-structured precision layering, this enables high throughput on MXUs while preserving numerical stability. In practice, the quantization and dequantization of blocks take up negligible computation time.

## 4 Results

### 4.1 Hardware and Software Specifications

We evaluated our implementation on two high-end GPU platforms: the NVIDIA H200 and the AMD MI300X. In the current work, we focus on single-GPU evaluation only. All benchmarks were conducted using Julia 1.12.0, with GPU support enabled via CUDA.jl (v5.9.5), AMDGPU.jl (v2.1.4), KernelAbstractions.jl (v0.9.39), and GPUArrays.jl (v11.3.1). Our Julia-based implementation is fully portable across vendors, with performance-critical kernels dispatching to either NVIDIA’s cuBLAS/cuSOLVER or AMD’s rocBLAS/hipSOLVER backends, depending on the target device.

For our benchmarks, we generated dense, symmetric positive-definite matrices with random uniform entries. To ensure positive definiteness and robust conditioning, we added  $n$  to the diagonal elements of the matrix.

## 4.2 Results Analysis on NVIDIA H200

We denote precision configurations as ordered lists from the outermost (largest off-diagonal) to the innermost (diagonal) recursion level. For instance, [FP16, FP32] assigns FP16 to the off-diagonal block and FP32 to the diagonal blocks.

*SYRK Performance.* Figure 4 reports the speedup of our Julia-based nested recursive SYRK implementation on the NVIDIA H200 GPU, normalized against cuBLAS SYRK in FP64. As the matrix size increases, our recursive kernel consistently outperforms cuBLAS across all precision configurations. The FP64 variant already achieves up to a  $14\times$  speedup at  $n = 65,536$ , benefiting from increased concurrency and improved reuse of tile-local data. The Pure F16 configuration exposes the hardware’s peak throughput, reaching a  $149\times$  speedup. By selectively exploiting this low-precision performance, mixed-precision layouts such as [FP16, FP16, FP32] achieve more than  $19\times$  acceleration, while the five-layer configuration [FP16, FP16, FP16, FP16, FP32] delivers up to  $27\times$  speedup with practical accuracy.

*TRSM Performance.* Figure 5 shows the speedup of our Julia-based recursive TRSM implementation on the NVIDIA H200 GPU, normalized to cuBLAS TRSM in FP64 (baseline = 1.0). For smaller matrices, all precision configurations perform similarly to the FP64 baseline. As the matrix size increases, our recursive and mixed-precision variants begin to clearly outperform cuBLAS. The Pure F16 implementation achieves the highest throughput, reaching up to  $6\times$  speedup at  $n = 65,536$ . Layered mixed-precision hierarchies such as [F16, F16, F16, F16, F32] still provide substantial gains, delivering up to  $5.3\times$  acceleration while offering better numerical robustness than pure FP16.

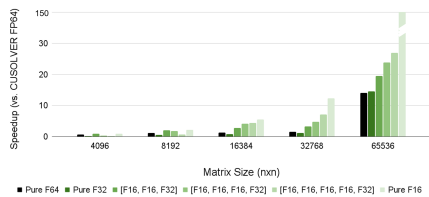


**Fig. 4.** Speedup of Recursive SYRK on NVIDIA H200. Relative performance of the recursive Symmetric Rank-k update compared to cuBLAS FP64.

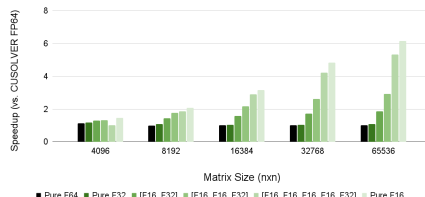


**Fig. 5.** Speedup of Recursive TRSM on NVIDIA H200. Performance of the recursive Triangular Solve normalized to cuBLAS FP64.

*Cholesky Throughput.* Figure 6 reports the Cholesky throughput on the NVIDIA H200, showing the effective TFLOP/s achieved by our recursive solver across matrix sizes and comparing it against cuSOLVER FP64. For large problems (e.g.,  $n = 65,536$ ), the FP64 and FP32 recursive variants already match or

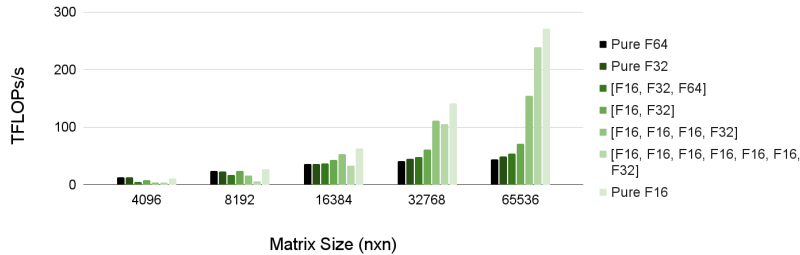


**Fig. 6.** Cholesky Throughput on NVIDIA H200. Effective TFLOPs across matrix sizes.

slightly exceed the cuSOLVER FP64 throughput. The triple-precision [F16, F32, F64] configuration provides an intermediate boost, reaching roughly 54 TFLOP/s. Meanwhile, the deep mixed-precision configuration [F16, F16, F16, F16, F16, F32] reaches more than 5× the FP64 cuSOLVER rate. The **Pure F16** implementation attains the highest raw throughput overall, approaching 6× the FP64 baseline, demonstrating how hierarchical mixed precision can fully exploit the H200’s MXUs for Cholesky factorization. At the same matrix size, both cuSOLVER FP64 and our recursive FP64 achieve roughly 65% of the peak FP64 Tensor Core performance, whereas **Pure F16** reaches about 30% of the theoretical FP16 peak. This drop in efficiency at lower precision reflects a shift in the bottleneck: as computation becomes cheaper, the algorithm increasingly becomes limited by memory bandwidth and data movement overhead rather than flops. In this regime, our deepest mixed-precision configuration [F16, F16, F16, F16, F16, F16, F16, F32] sustains about 22% of the FP16 peak, yet remains roughly two orders of magnitude more accurate than **Pure F16**. Together, these results highlight that peak utilization alone is not the right objective: carefully layered mixed precision can trade a modest reduction in hardware efficiency for dramatically improved accuracy while still delivering multi× speedup over the standard high-precision solver.

*Cholesky Performance.* Our performance evaluation of Cholesky factorization on the NVIDIA H200 GPU (Fig. 7) highlights the benefit of precision-aware recursion. All results are normalized against cuSOLVER’s FP64 performance (baseline = 1.0). Shallow configurations [F16, F32] yield modest speedups, and the [F16, F32, F64] configuration overcomes initial small-matrix overhead to reach a 1.21× speedup. Deeper mixed-precision hierarchies, such as [F16, F16, F16, F32] and [F16, F16, F16, F16, F16, F16, F32], show progressively higher gains—reaching over 4× and 5× speedups respectively for large matrices ( $n = 65,536$ ). The deepest configuration (**Pure F16**) achieves nearly 6× acceleration, highlighting the synergy between low-precision arithmetic and our recursive implementation. These gains stem from the aggressive use of fast FP16 compute and efficient tiling strategies that exploit the H200’s high memory bandwidth and ample L2 cache.

We can break down the execution time of the full FP64 recursive solver at  $n = 65,536$ , which has a runtime of 2,141 ms. The recursive TRSM and SYRK updates account for roughly 788 ms (37%) and 514 ms (24%) of the total runtime, respectively. The remaining 839 ms (39%) is spent in the POTRF base cases and recursive overhead. Because the TRSM and SYRK off-diagonal updates account for over 60% of the execution time, accelerating the performance of these specific routines via low-precision is what drives the speedups observed in large matrices.

*Cholesky Accuracy.* Figure 8 reports the accuracy of our mixed-precision Cholesky factorizations on the H200 GPU. It shows the relative error norm between the Cholesky factor computed using each mixed-precision configuration and the baseline FP64 result, plotted across matrix sizes. Note that we report the factorization error ( $\|A - LL^T\|/\|A\|$ ) rather than the residual error of a solved system, as it provides a more conservative measure of numerical stability. As expected, **Pure F64** attains the highest accuracy, with more than 15 correct digits. The configuration **[F32, F32, F32, F64]** remains very close, preserving roughly 12 digits and outperforming **Pure F32**, which yields about 8 digits. Introducing FP16 at the lower levels (**[F16, F32]**) still maintains single-precision-like accuracy (around 7–8 digits), while delivering substantial speedups in our performance results. For applications requiring strict reliability, adding a top layer of FP64 (**[F16, F32, F64]**) tightly tracks the **Pure F64** baseline accuracy while still offering performance gains. Deeper hierarchies with more FP16 (**[F16, F16, F16, F32]** and **[F16, F16, F16, F16, F16, F32]**) gradually reduce accuracy to about 5–6 digits, yet remain markedly more accurate than **Pure F16**, which drops below 4 digits. Overall, this illustrates a clear trade-off: the deepest configuration (**[F16, F16, F16, F16, F16, F16, F32]**) achieves a  $5.32\times$  speedup but retains only 5–6 digits of accuracy, whereas the **[F16, F32, F64]** configuration reaches roughly 9 digits of accuracy but with a more modest  $1.21\times$  speedup.

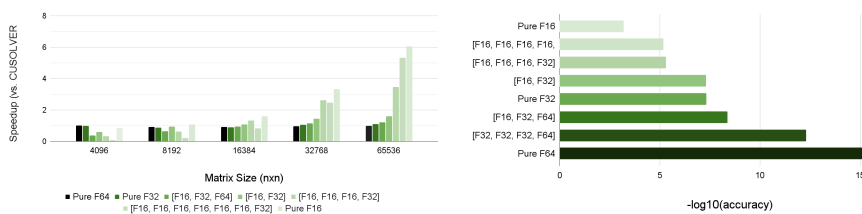


**Fig. 7.** Cholesky Speedup on NVIDIA H200. Performance of the full nested recursive solver compared to cuSolver FP64. **Fig. 8.** Cholesky Accuracy on NVIDIA H200. Relative error norms ( $-\log_{10}$ ) various precision configurations.

### 4.3 Results Analysis on AMD MI300X

We evaluate our recursive Cholesky solver on the AMD MI300X, using vendor-optimized `rocSOLVER` FP64 as the baseline. Figure 9 shows the speedup over `rocSOLVER` across matrix sizes, where higher bars indicate better performance.

The first three bars correspond to uniform precision: FP64, FP32, and FP16. Our FP64 solver matches `rocSOLVER` accuracy while achieving up to  $1.5\times$  speedup at  $n = 65,536$ , thanks to recursive blocking and improved cache reuse on MI300X. The FP32 and FP16 variants achieve up to  $2.1\times$  and  $3.8\times$  speedups respectively, though FP16 suffers in accuracy. The remaining bars represent mixed-precision variants with increasing layering depth. The [FP32, FP64] configuration improves performance while preserving stability, reaching  $2.5\times$  speedup. The [FP16, FP32, FP64] and [FP16, FP16, FP32] variants further raise speedup to  $4\times$  and beyond. Our deepest layout, [FP16, FP16, FP16, FP32], achieves up to  $5.3\times$  speedup, balancing MXU throughput with acceptable accuracy.

These results confirm that our recursive, mixed-precision solver outperforms `rocSOLVER` for large matrices across all tested configurations, while enabling fine-grained control over performance–accuracy tradeoffs.

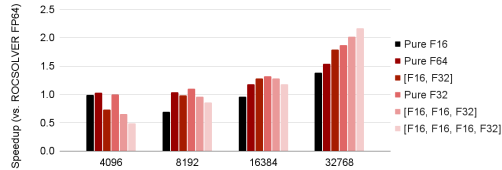


**Fig. 9.** Cholesky Speedup on AMD MI300X. Performance compared to `ROC SOLVER` FP64.

#### 4.4 Effect of Recursive Depth and Matrix Scale

One of the key advantages of utilizing a nested recursive formulation is the ability to tune the performance and accuracy by changing the number of levels of recursion. As shown in Figure 11, the speedup of the best mixed-precision configuration scales linearly with matrix size, reaching a peak of  $5.32\times$  at  $n = 65,536$ . This trend is driven by the fact that larger matrices allow for deeper recursion hierarchies while maintaining leaf block sizes large enough to run efficiently on hardware. At these larger scales, increasing the recursive depth maximizes the proportion of floating-point operations that occur in the off-diagonal blocks, which are computing with FP16 GEMM operations. However, this strategy is less effective on smaller matrices; if the recursion is too deep relative to the matrix size, the blocks become too small, and the overhead of managing many tiny tasks outweighs the computational benefits.

#### 4.5 Results on Real-World Matrices and Limitations

We evaluated our mixed-precision nested recursive Cholesky algorithm on real-world matrices using datasets from the SuiteSparse Matrix Collection, accessed via the Julia `MatrixDepot` package on an NVIDIA GPU. One key matrix we evaluated was `Pothen/bodyy5`, a sparse, symmetric positive-definite matrix derived from NASA structural engineering data ( $n = 18,589$ ). As shown in Figure 10, mixed precision retains high accuracy for moderately conditioned matrices like

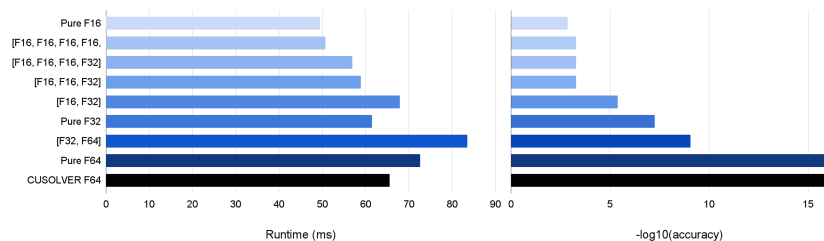


**Fig. 10.** Performance and accuracy of mixed-precision configurations on the `body5` matrix on NVIDIA H200 GPU. Runtime (left) and relative error (right) demonstrate that mixed-precision configurations achieve substantial speedups while maintaining numerical stability.

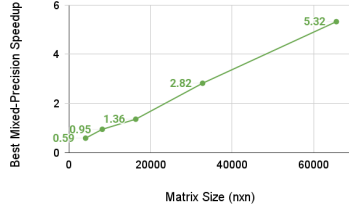
`body5`. Our blockwise quantization effectively scales the values to prevent immediate overflow. We notice that as the precision increases from FP16  $\rightarrow$  FP32  $\rightarrow$  FP64, the runtime correspondingly increases because higher precision arithmetic requires more computational resources and memory bandwidth. Mixed-precision configurations such as [F16, F32] and [F16, F16, F32] provide an intermediate performance point, achieving substantial speedups compared to pure FP64 while maintaining greater numerical stability than pure FP16.

However, the solver does face limitations with certain real-world matrices. For small matrices ( $n < 16,000$ ), as Figure 11 suggests, the solver does not perform as effectively due to the type conversion overhead. The strategy also provides the best results for diagonally dominant matrices. Furthermore, matrices that possess extreme dynamic ranges are not well-suited for an in-place solver either. For example, `Simon/raefsky4` ( $n = 19,779$ ) has a dynamic range exceeding  $10^{11}$ . When applying quantization to a matrix like this, the scaling process compresses the massive values down so severely that it causes underflow, crushing the lower values to zero. This destroys the positive definiteness of the sub-blocks, eventually causing division by zero and NaN propagation. Therefore, static blockwise quantization is insufficient for these cases, and future work should explore more dynamic quantization schemes.

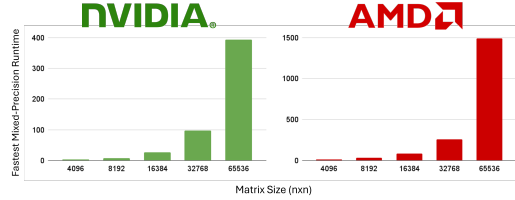
#### 4.6 Portability and impact of hardware

Figure 12 shows the runtime of the fastest mixed-precision scenarios at each data size for the NVIDIA H200 and AMD MI300X GPUs, demonstrating the portability of our implementation: with a single high-level algorithmic implementation, we cover all GPU hardware backends by using multi-dispatch to direct the base case functions to the optimized vendor library implementations. Several factors contribute to the lower performance observed on AMD compared to NVIDIA hardware, including the performance of the optimized base cases and the inclusion of mixed-precision matrix multiplication (`GemmEx`). For this benchmark, we included mixed-precision matrix multiplication for NVIDIA, but not

for AMD hardware, due to its unavailability at the time in the Julia ecosystem. Future work into fully hardware-agnostic mixed-precision GEMM operations could address this and render the entire algorithm lifecycle hardware-agnostic, potentially unlocking new levels of performance not only on AMD hardware, but also on Apple Metal GPUs.



**Fig. 11.** Speedup Scaling with Matrix Size on NVIDIA hardware. Performance gains improve substantially as the matrix grows, allowing for deeper recursion levels.



**Fig. 12.** Cross-Platform Portability. Best mixed-precision speedup on NVIDIA H200 and AMD MI300X.

## 5 Conclusion and Future Work

We presented a high-performance, mixed-precision solver for symmetric linear systems based on a nested recursive Cholesky decomposition that uniformly applies recursion across POTRF, TRSM, and SYRK phases. This design exposes a rich hierarchy of GEMM operations, which maps efficiently onto matrix processing units (MXUs) such as NVIDIA Tensor Cores and AMD Matrix Cores. We introduced the first recursive GPU implementation of SYRK and demonstrated that recursive TRSM and SYRK enable deeper task decomposition and fine-grained parallelism. Our implementation in Julia leverages multiple dispatch, array abstractions, and dynamic type inference to enable layered precision control and backend portability across GPU architectures. The solver achieves substantial speedups over high-precision baselines while maintaining better numerical accuracy than low-precision calculations—realizing over  $5\times$  speedup on NVIDIA H200 and exhibiting similar gains on AMD MI300X. We have also demonstrated the utility of the mixed-precision strategy on a real-world example dataset. The strategy proposed in this work is best suited for matrices that are diagonally dominant, reasonably large, and with limited dynamic range. Future work could focus on extending the strategy to other classes of matrices by exploring other mixed-precision and quantization schemes.

While this work focuses on dense symmetric positive-definite systems, we envision extending our recursive and mixed-precision strategy to broader classes of linear algebra problems. These include block-sparse and banded systems, as well as  $LDL^T$  factorizations for indefinite matrices. Further, the recursive GEMM structure opens avenues for hardware-aware autotuning, energy-efficient

scheduling, and integration with asynchronous task-based runtimes. Incorporating adaptive precision control based on condition number estimates and expanding support for hierarchical memory systems are also promising directions. Finally, extending this framework towards a multi-GPU implementation as in large-scale linear algebra libraries [32] could unlock performance benefits at even larger scales. Thanks to the hierarchical abstract data structure, adaptation of the algorithm for heterogeneous hardware [1] can also be directly integrated.

**Acknowledgments** We would like to extend our gratitude for the work and support of members of the Julia Lab, in particular Tim Besard, Julian Samaroo, and Valentin Churavy, who developed and helped with our understanding of available tools within the Julia ecosystem for performance portability. R.A. acknowledges the KAUST Ibn Rushd post-doctoral fellowship. The authors acknowledge the MIT Office of Research Computing and Data, ACES at Texas A and M HPRC (CIS250776 ACCESS, supported by U.S. NSF 2138259, 2138286, 2138307, 2137603, 2138296), and the Advanced Micro Devices Developer Cloud for providing high-performance computing resources. This material is based upon work supported by the US NSF (CNS-2346520, PHY-2028125, RISE-2425761, DMS-2325184, OAC-2103804, OSI-2029670), DARPA (HR00112490488), DoE (DE-NA0003965), and USAFR (FA8750-19-2-1000). The U.S. Government, its agencies, and their employees do not make any warranty, do not endorse, recommend, or favor, nor assume any liability for anything in this report, nor represent that its use would not infringe privately owned rights. The views and opinions expressed herein are those of the authors only.

## References

1. Agullo, E., Beaumont, O., Eyraud-Dubois, L., et al.: Bridging the gap between performance and bounds of Cholesky factorization on heterogeneous platforms. In: Proc. IPDPS Workshops. pp. 34–45 (2015). <https://doi.org/10.1109/IPDPSW.2015.35>
2. Akbudak, K., Ltaief, H., Mikhalev, A., Keyes, D.: Tile low rank Cholesky factorization for climate/weather modeling applications on manycore architectures. In: Proc. ISC High Performance. pp. 22–40. Springer (2017)
3. Alomairy, R., Abdulah, S., Cao, Q., Genton, M.G., Keyes, D.E., Ltaief, H.: Sustainably modeling a sustainable future climate. In: Proc. HPEC. pp. 1–8. IEEE (2025)
4. Alomairy, R., Cao, Q., Ltaief, H., Keyes, D., Edelman, A.: Scalable Hamming distance computation using accelerated matrix transformations. In: Proc. ISC High Performance. pp. 1–13 (2025)
5. Alomairy, R., Tome, F., Samaroo, J., Edelman, A.: Dynamic task scheduling with data dependency awareness using Julia. In: Proc. HPEC. pp. 1–7. IEEE (2024)
6. Alomairy, R.M.: High-performance scientific applications using mixed precision and low-rank approximation powered by task-based runtime systems. Ph.D. thesis, KAUST (2022)
7. Amestoy, P.R., et al.: Mixed precision low-rank approximations and their application to block low-rank LU factorization. *IMA J. Numer. Anal.* **43**(4), 2198–2227 (2023)

8. Andersen, B.S., Waśniewski, J., Gustavson, F.G.: A recursive formulation of Cholesky factorization of a matrix in packed storage. *ACM Trans. Math. Softw.* **27**(2), 214–244 (2001)
9. Anderson, E., et al.: *LAPACK Users' Guide*. SIAM (1999)
10. Baboulin, M., et al.: Accelerating scientific computations with mixed precision algorithms. *Computer Physics Communications* **180**(12), 2526–2533 (2009)
11. Ballard, G., Demmel, J., Holtz, O., Schwartz, O.: Communication-optimal parallel and sequential Cholesky decomposition. In: *Proc. SPAA '09*. pp. 245–252 (2009). <https://doi.org/10.1145/1583991.1584054>
12. Bezanson, J., Edelman, A., Karpinski, S., Shah, V.B.: Julia: A fresh approach to numerical computing. *SIAM Review* **59**(1), 65–98 (2017)
13. Bosilca, G., Ltaief, H., Dongarra, J.: Power profiling of Cholesky and QR factorizations on distributed memory systems. *Computer Science – Research and Development* **29**(2), 139–147 (2014)
14. Buttari, A., et al.: Mixed precision iterative refinement techniques for the solution of dense linear systems. *Int. J. High Perform. Comput. Appl.* **21**(4), 457–466 (2007)
15. Cao, Q., et al.: Reducing data motion and energy consumption of geospatial modeling applications using automated precision conversion. In: *Proc. IEEE CLUSTER* (2023)
16. Carrica, V., Alomairy, R., Ringoot, E., Edelman, A.: Accelerating linear solve with mixed precision nested recursive subdivision on AI hardware (2025), sC25 Poster
17. Carrica, V., Onyango, M., Alomairy, R., Ringoot, E., Schloss, J., Edelman, A.: Toward portable GPU performance: Julia recursive implementation of TRMM and TRSM. arXiv preprint arXiv:2504.13821 (2025)
18. Carson, E., Higham, N.J.: A new analysis of iterative refinement and its application to accurate solution of ill-conditioned sparse linear systems. *SIAM J. Sci. Comput.* **39**(6), A2834–A2856 (2017)
19. Carson, E., Higham, N.J.: Accelerating the solution of linear systems by iterative refinement in three precisions. *SIAM J. Sci. Comput.* **40**(2), A817–A847 (2018)
20. Charara, A., Keyes, D., Ltaief, H.: A framework for dense triangular matrix kernels on various manycore architectures. *Concurrency and Computation: Practice and Experience* **29**(15), e4187 (2017)
21. Chen, C., Martinsson, P.G.: Solving linear systems on a GPU with hierarchically off-diagonal low-rank approximations. In: *Proc. SC22*. pp. 1–15. IEEE (2022)
22. Eliahu, D., Spillinger, O., Fox, A., Demmel, J.: Frpa: A framework for recursive parallel algorithms. Tech. rep., EECS, University of California at Berkeley (2015)
23. Faverge, M., et al.: Programming heterogeneous architectures using hierarchical tasks. *Concurrency and Computation: Practice and Experience* **35**(25), e7811 (2023)
24. Furmento, N., et al.: Optimizing parallel heterogeneous system efficiency: Dynamic task graph adaptation with recursive tasks. *J. Parallel Distrib. Comput.* **205**, 105157 (2025)
25. Gardner, J., Pleiss, G., Weinberger, K.Q., Bindel, D., Wilson, A.G.: GPyTorch: Blackbox matrix-matrix Gaussian process inference with GPU acceleration. *Advances in Neural Information Processing Systems* **31** (2018)
26. Giordano, M., Klöwer, M., Churavy, V.: Productivity meets performance: Julia on A64FX. In: *Proc. IEEE CLUSTER*. pp. 549–555 (2022)
27. Grasedyck, L., Kriemann, R., Le Borne, S.: Domain decomposition based H-LU preconditioning. *Numerische Mathematik* **112**(4), 565–600 (2009)

28. Haidar, A., Tomov, S., Dongarra, J., Higham, N.J.: Harnessing GPU tensor cores for fast FP16 arithmetic to speed up mixed-precision iterative refinement solvers. In: Proc. SC18. pp. 603–613. IEEE (2018)
29. Higham, N.J., Mary, T.: Mixed precision algorithms in numerical linear algebra. *Acta Numerica* **31**, 347–414 (2022)
30. Lang, J., Guo, Z., Huang, S.: A comprehensive study on quantization techniques for large language models. In: Proc. ICAIRC. pp. 224–231. IEEE (2024)
31. Ltaief, H., Alomairy, R., Cao, Q., et al.: Toward capturing genetic epistasis from multivariate genome-wide association studies using mixed-precision kernel ridge regression. In: Proc. SC24. pp. 1–12. IEEE (2024)
32. Ltaief, H., Tomov, S., Nath, R., Du, P., Dongarra, J.: A scalable high performant Cholesky factorization for multicore with GPU accelerators. In: Proc. VECPAR 2010. pp. 93–101. Springer (2011)
33. Piscaglia, F., Ghioldi, F.: GPU acceleration of CFD simulations in OpenFOAM. *Aerospace* **10**(9), 792 (2023)
34. Ren, J., Ltaief, H., Abdulah, S., Keyes, D.E.: Accelerating mixed-precision out-of-core cholesky factorization with static task scheduling. In: ISC High Performance 2025 Research Paper Proceedings (40th International Conference). pp. 1–12. Prometheus GmbH (2025)
35. Ringoot, E., Alomairy, R., Edelman, A.: A GPU-resident memory-aware algorithm for accelerating bidiagonalization of banded matrices. arXiv preprint arXiv:2510.12705 (2025)
36. Tomanović, I., et al.: CFD code parallelization on GPU and the code portability. *Advanced Theory and Simulations* **8**(3), 2400629 (2025)
37. Van Zee, F.G., et al.: The libflame library for dense matrix computations. *Computing in Science & Engineering* **11**(6), 56–63 (2009)
38. Zhang, Q., Alomairy, R., Wang, D., Gu, Z., Cao, Q.: Leveraging hardware-aware computation in mixed-precision matrix multiply: A tile-centric approach. In: Proc. WAMTA. pp. 174–185. Springer (2025)